Novel Real-Time Decision-Based Carrier Tracking for Software-Defined Radios Using M-ARY QAM Modulation

Nikhil Marriwala, University Institute of Engineering and Technology, Kurukshetra University, India*

(iD) https://orcid.org/0000-0002-1093-630X

Gnana Kousalya C., St. Joseph's Institute of Technology, India

B. Rajasekar, Sathyabama Institute of Science and Technology, Chennai, India

(iD) https://orcid.org/0000-0003-1182-848X

N. M. Nandhitha, Sathyabama Institute of Science and Technology, India

Ashu Gautam, G.D. Goenka University, India

Aarti Sangwan, Central University of Haryana, Mahendergarh, India

ABSTRACT

In this paper, a scalable and real-time decision-based carrier tracking for software defined radio (SDR) for M-ary QAM modulation has been proposed and tested in real-time using the universal software radio peripheral (USRP)-2922. The proposed system provides real-time decision-based carrier tracking for improved efficiency and performance. The real-time transfer of data has been done using the USRP-2922 hardware using the M-ary QAM modulation scheme for data transmission. The novelty of the proposed system is that one can transfer random data (binary bits), text or an image which can be encoded using the desired forward error correction codes (FEC) namely the convolution coding/ Viterbi soft decision decoding and the turbo coding/decoding. The proposed novel SDR transceiver system with real-time decision-based carrier tracking shows an improved performance for different parameters such as the bit error rate (BER) and signal to noise ratio (Eb/No).

KEYWORDS

Bit Error Rate, Convolution coding, Decision-Based SDR, Carrier Tracking, FEC Codes, Graphical User Interface, M-QAM, Turbo coding

1. INTRODUCTION

SDR refers to the technology where software modules are designed and run on a generic platform made up of digital signal processors and many general-purpose microprocessors used to employ

different radio functions like modulation (generation of signal to be transmitted) at the transmitter and demodulation (tuning/detection) of the received signal at the receiver (Yarkan 2015). A wide range of radio applications including the wireless local area network (WLAN), global positioning system (GPS), Bluetooth etc. can be implemented using the SDR technology (Javornik et al., 2005). With the new development of different ways and means by which people communicate (Mitola et al., 1999). SDR technology brings flexibility in the system, cost efficiency, multi-user communication. SDR provides so many benefits to the end-user realized by service providers and product developers (Tribble, 2008). SDR system has the capability of replacing traditional hardware which is still in common use like the FM radio or TV transmission as it can adapt to a variable environment for many different applications (Adachi & Parsons, 1989). SDR system offers a very promising futuristic technology that reduces the hardware cost as it can replace systems like FM radio or TV broadcast and cellular communication systems (Moir & Pettigrew, 2014). SDR system is an advantageous, adjustable and future-proof solution to deploy both existing and emerging standards (Sampaio, Gomes, & Santos, 2012). An SDR system provides reconfigurability, intelligence and capability to program hardware with software upgrades (Mitola, 1999). Moreover, it can provide global seamless connectivity and also provides the solution to interoperability (Note & Advanced, 2005). In a nutshell, SDR is a technology that offers multi-mode, multi-modulation reconfigurable and future-proof environment.

The proposed SDR transceiver system can be used in real-time conditions for the transfer of the data in different forms such as binary codes or text and image. As the proposed system uses M-QAM for modulation of the data it shows a better performance for lower modulation order whereas the out gets inferior as we move to a higher order of 'M'. The proposed system uses FEC codes makes the system more secure and future-ready. The proposed SDR transceiver system uses decision-based carrier tracking which ensures that phase tracking routine, the phase error, affected by the initial phase and frequency difference, is minimized and the received signal becomes a perfect reproduction of the transmitted signal except for the time delay. The biggest advantage of the proposed SDR transceiver system is that it is built as a reconfigurable system that can perform real-time signal processing. The proposed SDR transceiver system is generic in nature and offers a low-cost solution for secured transmission of data in real time. As the proposed SDR transceiver system runs on a generic platform it is easier to optimize the processing of the signal/data. In the proposed generic SDR transceiver system the complete processing of the Signal/data has been successfully performed through software. The dedicated hardware's used for testing the performance of the proposed SDR transceiver system; perform only the down conversion and digitization of a wide band of the RF spectrum. The proposed SDR helps to exploit the flexibility of signal/data processing through software thus helping to realize a system which could be modified dynamically at any stage through software.

2. RELATED WORK

In global system for mobile communication (GSM) (Schiller, 2003), gaussian minimum shift keying (GMSK) (Liu, 2006) is used (GMSK is a form of continuous-phase frequency shift keying). In general packet radio service (GPRS)(Schiller, 2003), 8-phase shift keying (8PSK) is used. Many users in GPRS and GSM can be given the right to use the network by making use of the time division multiple access (TDMA) or the frequency division multiple access (FDMA) schemes. Another modulation scheme that offers many benefits is code division multiple access (CDMA) (Kunisawa et al., 2007) modulation which is used in standards like IS-95 and UMTS (Valenti & Sun, 2001) (a competitor to GSM and GPRS). In CDMA information bits are modulated using a higher rate sequence of pseudorandom bits called PN sequence. PN sequences are generated to be orthogonal to each other. This allows multiple users to use the time-frequency medium at the same time.

For any dependable communication system, FEC codes (Marriwala, Sahu, & Vohra, 2016b) are the main part of it. FEC is a method of adding redundant bits to the information to be sent from the transmitter to help the receiver correct errors (Marriwala, Sahu, & Vohra, 2013). The FEC codes

are divided into two types namely the Convolutional codes and block codes (Fellenberg & Rohling, 2009) (Marriwala, Sahu, & Vohra 2016a). Claude Shannon (Shannon, 1948) proposed the coding theory based on "the mathematical theory of communication." Claude Shannon gave the theory that the data can be transmitted without errors if the *channel capacity* is higher than the bit rate.

Shannon proved that by the use of appropriate codes errors can be removed from the message signal received. The error-free codes can be termed *block codes*. Block codes are the ones where the redundancy is added to blocks of the data. The *convolutional codes* are the codes in which the redundancy is added continuously (Fleming, 2002). The Viterbi decoder can be used to decode the Convolutional codes(Marriwala et al., 2016b). This can be done using a soft Viterbi decoder also. Another method for error-free decoding is through the use of Turbo codes (Bhanubhai, Shajan, & Dalal, 2012) and LDPC codes. The turbo codes have shown a performance very near to the Shannon limit. The turbo codes use numerous iterative decoding algorithms such as the Gallager's low parity density check (LDPC) codes (Borle, Zhao, & Chen, 2014). Fepeussi et al. has proposed a mixed-integer linear programming model manages front-ends which ties together the technique of time-division sharing (Fepeussi et al., 2019). (Molla et al., 2022) has provided a list of well-known general purpose processor (GPP) based SDR platforms, which satisfy the minimum specifications of selected wireless standards. In this paper, the authors have reviewed the characteristics of selected wireless technologies. The paper investigates different SDR platform architecture and their maximal performance in terms of the frequency range; bandwidth, symbol rate, bitrate, and latency support (Molla et al., 2022). (Kumar, Rawat, & Rawat, 2020) in their paper have proposed a software-defined radio (SDR) based transceiver system which is designed and implemented on the system-on-chip (SoC) platform. The proposed system consists of a high-speed Arm embedded processor and a reconfigurable field-programmable gate array (FPGA) which Implements the real-time baseband signal generation and adaptive digital predistortion (ADPD) units on the SoC platform (Kumar et al., 2020). The proposed SDR transceiver design by(Bloessl et al., 2018) provides access to all data down to and including the physical layer, allowing for a better understanding of the system. The proposed transceiver design can be modified and is completely transparent as it is based on open and programmable hardware and software.

3. ABOUT THE USRP HARDWARE

USRP is an SDR platform that provides the developers and researchers to perform real-time transfers of data and visualize the performance of the algorithms developed by them (Gandhiraj & Soman, 2014). The USRP is an RF-based radio transceiver that can be programmed through software and which is developed and designed for research in the field of new Wireless technologies. NI USRP-2922 SDR transceiver has been used in the real-time testing of the proposed transceiver for SDR. The NI USRP-2922 hardware has been programmed using LabVIEW. The NI USRP-2922 provides an RF platform that is a reasonably priced, cost-effective easy-to-use prototype for wireless applications such as physical layer communication, spectrum monitoring, and many more. The block diagram of the USRP module used for real-time testing of the system is shown in Figure 1. The USRP-2922 uses two separate transmit and receive signal chains. The specification of the NIUSRP-2922 is given in Table 1.

4. QAM MODULATION

As it has been observed that the QAM modulation scheme is being widely used for data transmission applications over bandpass channels hence it has been chosen to be the modulation scheme of the proposed SDR transceiver system. Figure 2 represents the QAM modulation process. It uses two separate product modulators as shown in Figure 2 and two carriers of the same frequency which differ in phase by -90^0 [19]. The multiplexed signal *s(t)* consists of the sum of these two product modulator outputs as shown by equation (1):-

Table 1. Specification for USRP-2922

Range of Frequency	400 MHz to 4.4 GHz
Frequency step	**<1 kHz**
Output Power (Max)	(Pout)50 mW to 100 mW (17 dBm to 20 dBm)
Range of Gain	0 dB to 31 dB
Gain Step	05 dB
Accuracy of Frequency	25 ppm
Instantaneous Bandwidth (Max.) in real-time	16-bit sample width20 MHz 8-bit sample width40 MHz
'I/Q' sampling rate (Max.)	16-bit sample width25 MS/s 8-bit sample width50 MS/s
DAC2 channels	400 MS/s, 16 bit
DAC SFDR	80 dB

Figure 1. USRP system block diagram
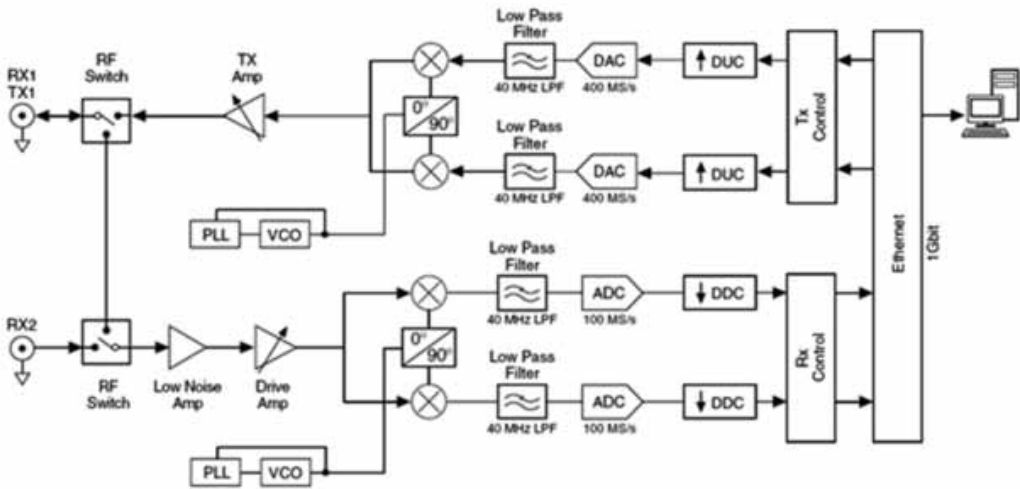
$$s(t) = A_c m_1(t) \cos(2\pi f_c t) + A_c m_2(t) \sin(2\pi f_c t) \tag{1}$$

Where, $m_1(t)$ and $m_2(t)$ = Two different message signals are given to the product modulator.

The two paths to the adder are typically referred to as the 'I' (in-phase), and 'Q' (Quadrature) arms.

4.1 Bit Error Probability of M-QAM

The QAM digital modulation scheme can allow sending two different signals at the same time using the same carrier frequency, with one shifted by 90° concerning others. The transmitted signal is represented by equation (2):

$$S(t) = d_1(t) \cos 2\pi f_c t + d_2(t) \sin 2\pi f_c t \tag{2}$$

Figure 2. QAM Modulation Process
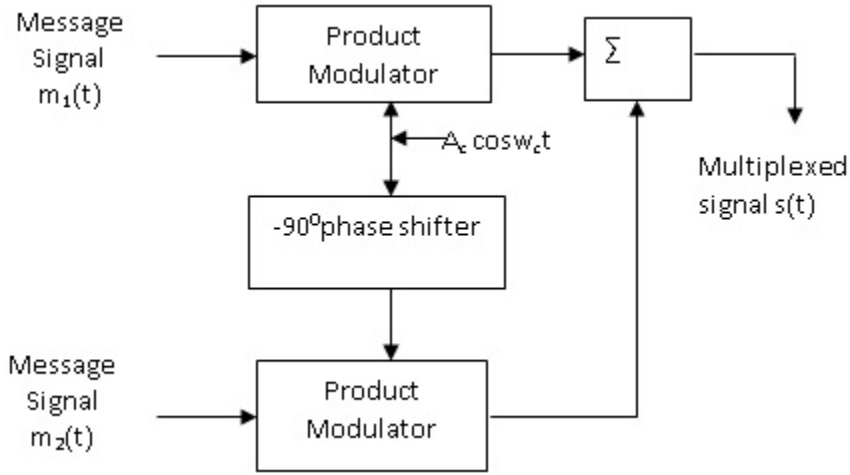
Equation (3) represents the average probability of error for an AWGN channel using the M-ary QAM using coherent detection

$$p_b = 2 / logM \left\{ M^{1/2} - 1 / M \log M^{1/2} \right\} \left[1 - \mathrm{erf} \sqrt{3} \log_2 M / 2 (M-1) (E_b / N_0) \right] \tag{3}$$

Equation (4) describes the average signal energy E_{av}:

$$P_e \cong 4 \left(1 - 1 / \sqrt{M} \right) Q \left(\sqrt{3} E_{avn} / (M-1) N_0 \right) \tag{4}$$

Where, P_b is the probability of bit error and M is modulation order.

All the symbols in a QAM signal occupy the same spectral space. The spectral efficiency of QAM is therefore quite good.

4.2 Convolution Encoding

Convolutional encoding used with Viterbi decoding is one of the FEC techniques that is used in our system for error correction and removal of noise. Convolutional codes are described by two different parameters: the code rate (*k/n*) and the constraint length (K).Where, '*k*' is the number of bits into the Convolutional encoder, '*n*' is the number of channel symbol output by the Convolutional encoder in a given encoder cycle, 'K' is the "length" of the Convolutional encoder.

The number of encoder cycles that can be retained by the input bit and later used for encoding after it had first appeared at the input to the Convolutional encoder is indicated by the parameter'. The 'm' parameter is closely related to 'K'. The memory length of the encoder is described by the 'm' parameter. The encoded bits depend on the current k input bits and also on few past input bits. Convolutional codes are commonly specified by three parameters; (*n,k,m*)Where n = number of output bits;*k* = number of input bits;*m* = number of memory registers.

The generator matrix used for the proposed SDR transceiver having a rate of 2/3 convolutional encoder, is specified as

$$
\begin{matrix}
100100 & 011000 & & 44 & 30 \\
011100 & 101000 & = & 34 & 50 \\
110000 & 010000 & & 60 & 20
\end{matrix}
$$

The proposed system uses a rate 2/3 convolutional encoder represented by Figure 3. A constraint length equal to 4 is used. As shown in Figure 3, a memory element/ shift register is represented by '**D**'

For the proposed SDR transceiver system, y_{ij}, $0 \pounds j \pounds n\text{-}1$ denotes the j_{th} output of the convolutional encoder, in the i_{th} encoding instance. The maximum number of bits encoded that can be affected by a single input bit are denoted by Constraint length (K). Any buffered bits from the previous iteration are added to the beginning of the input bitstream before performing convolutional encoding. Output bitstream returns the convolutional-encoded code word. This parameter is wired to the Convolutional Decode VI to recover the input data stream. The final state returns the final state for the $k(K\text{-}1)$ shift registers as the right-aligned (least significant) $k(K\text{-}1)$ bits. Input bit-stream array (*Message Data*) is divided into chunks of length equal to the data length (k). The convolutional encoder design sequentially encodes each chunk and recombines the encoded data to return the output codeword in the output bitstream array. The number of iterations required in the design to complete the encoding process is given by equation (5)

$$
Floor \left[legnth \left(Message\ Data \right) / k \right] \tag{5}
$$

During the ith iteration, the chunk of k bits is represented by the *Message Data* vector given by the following equation (6):

$$
\mathcal{X}_i = \left[x_i^0\ x_i^1 \ldots x_i^{k-2}\ x_i^{k-1} \right]^T \tag{6}
$$

Figure 3. Convolutional Encoder having Rate 2/3
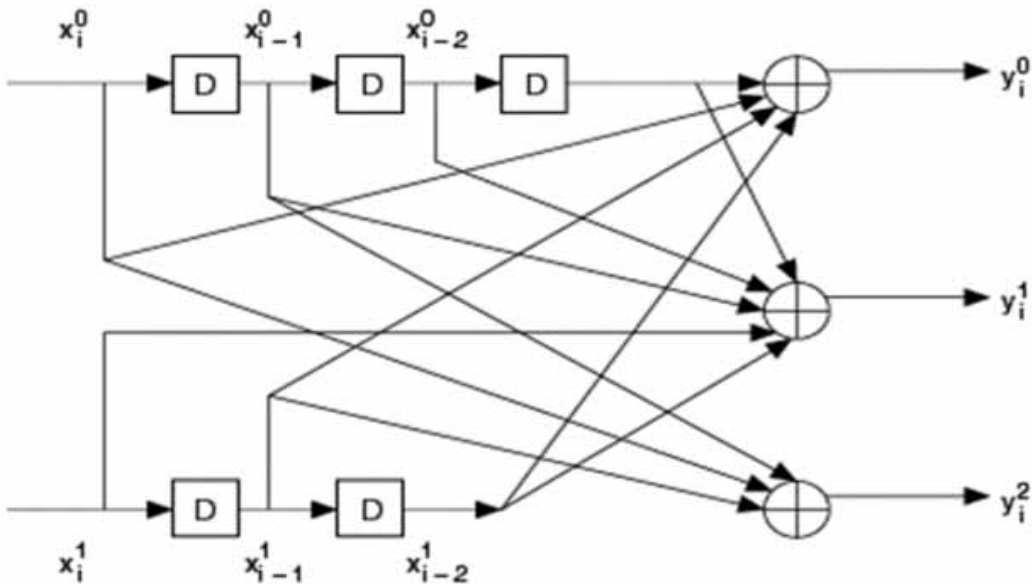
The corresponding output encoded vector is given by the equation (7):

$$\mathcal{Y}_i = \left[y_i^0 \, y_i^1 \cdots y_i^{n-2} \, y_i^{n-1} \right]^T \tag{7}$$

The output encoded vector is generated from the input message vector using the binary connection polynomial matrix G. The transformation can be described by the equation (8):

$$
\begin{bmatrix} y_i^0 \\ y_i^1 \\ \vdots \\ y_i^{n-1} \end{bmatrix}
=
\begin{bmatrix}
g_{0,0}^0 & g_{1,0}^0 & \cdots & g_{k-1,0}^0 & \cdots & g_{0,K-1}^0 & g_{1,K-1}^0 & \cdots & g_{k-1,K-1}^0 \\
g_{0,0}^1 & g_{1,0}^1 & \cdots & g_{k-1,0}^1 & \cdots & g_{0,K-1}^1 & g_{1,K-1}^1 & \cdots & g_{k-1,K-1}^1 \\
\vdots & \vdots & \vdots & \vdots & \vdots & \vdots & \vdots & \vdots & \vdots \\
g_{0,0}^{n-1} & g_{1,0}^{n-1} & \cdots & g_{k-1,0}^{n-1} & \cdots & g_{0,K-1}^{n-1} & g_{1,K-1}^{n-1} & \cdots & g_{k-1,K-1}^{n-1}
\end{bmatrix}
\begin{bmatrix}
x_i^0 \\ x_i^1 \\ \vdots \\ x_i^{k-1} \\ x_{i-1}^0 \\ x_{i-1}^1 \\ \vdots \\ x_{i-1}^{k-1} \\ \vdots \\ x_{i-(K-1)}^0 \\ x_{i-(K-1)}^1 \\ \vdots \\ x_{i-(K-1)}^{k-1}
\end{bmatrix}
\tag{8}
$$

The following section demonstrates the convolutional interleaving/deinterleaving. Figure 4 shows the convolution interleaver used for data input and output.

The data to be sent is say: x0, x1, x2, x3, x4, x5, x6, x7, x8, x9, x10, x11, x12, x13, …

D = unit delay in the path.

Figure 5 shows the convolution de-interleaver used for data input and output.

Interleaved Data received from the Interleaver: x0, 0, 0, 0, x4, x1, 0, 0, x8, x5, x2, 0, x12, x9, ….

The Deinterleaved Data received from the Deinterleaver: 0, 0, 0, 0, 0, 0, 0, 0, 0, 0, 0, 0, x0, x1, x2, x3, x4, x5, x6, x7, x8, x9,…

4.3 Viterbi Soft-Decision Decoder

The convolutional decoder receives the codewords as an array of values representing Boolean bits. The decoder applies the Viterbi hard decision decoding algorithm to obtain the maximum likelihood transmitted data sequence. The length N encoded input bitstream is first converted into a stream of encoded symbols of the length described by equation (9):

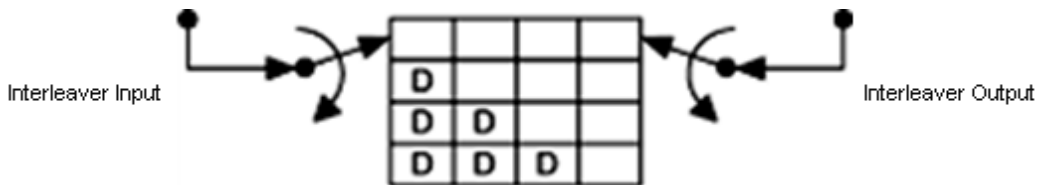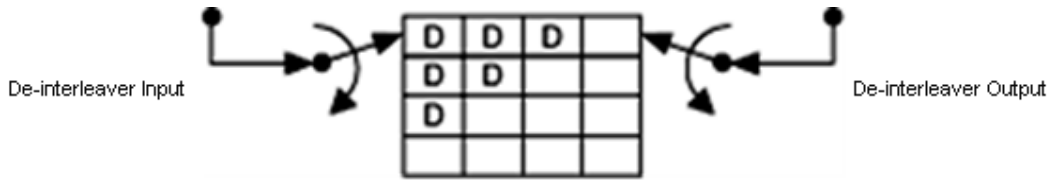**Figure 4. Convolution Interleaver used for data input and output**

Figure 5. Convolution Deinterleaver used for data input and output

$$Floor\left[legnth\left(input\ bitstream\right)/n\right] \quad\quad (9)$$

where n is the codeword length. Any bits truncated by the floor operation are buffered so that the VI can operate on a continuous stream of input bits. The Viterbi decoder processes D trellis stages before determining the maximum likelihood survivor path, where D represents the decoder traceback depth. Typical D values equal $5 \times K$ stages of the trellis, where K denotes the constraint length of the convolutional encoder. Viterbi decoding is implemented using the register exchange algorithm. For reduced computational overhead in determining the path and branch metrics, the VI uses $2^{(K-2)k}$ trellis elements of size 2^k elements during intermediate calculations. The following diagram represents binary soft symbol decisions from a demodulator. A sample close to -1 represents logic 1 while a sample closer to 1 represents logic 0.

In the Viterbi soft decision decoding, the decoder accepts unsigned integers. Additionally, it requires you to specify the number of soft-decision bits, n_{soft}, before decoding. These soft-symbol decisions are obtained by quantizing the soft binary symbol decisions to the specified bits of precision from the demodulator, as shown in Table 2. These unsigned integers range from 0 to $2^{n_{soft}}$. An eight-level quantization ($n_{soft} = 3$) yields less than a 0.25 dB reduction in gain received after coding relative to the unquantized Viterbi decoding. When $n_{soft} = 1$, the Viterbi soft-decision decoding algorithm reverts to performing hard-decision decoding. The following Table 2 describes the nature of inputs fed into the Viterbi Soft-Decision decoder. This Table 2 assumes that M-ary symbol decisions from the demodulator are quantized to 3 bits of precision.

Traceback depth (D) postulates the number of trellis stages used in the Viterbi decoding process and value of (D) used is 15.

4.4 Turbo Coding

The proposed SDR transceiver makes use of a turbo encoder which consists of a parallel concatenation of two Recursive Systematic Convolutional (RSC) codes separated by an inter leaver as shown in Figure

Table 2. Inputs fed into the Viterbi Soft-Decision Decoder

Soft Decision Input	Logic Value
0	Strong logic 0
1	Highly likely to be 0
2	Moderate 0
3	Uncertain (0 or 1)
4	Uncertain (0 or 1)
5	Moderate 1
6	Highly likely to be 1
7	Strong logic 1

6 which are 1/2 rate RSC encoders. A permutation function 'α' permutates the interleaved data received from the lower encoder which receives the data directly by the upper encoder. It is a pseudo-random inter leaver which is used to map bits in position i to position α(i) based on some prescribed randomly generated rule. The data of the bottom encoder is not transmitted whereas the data of the top encoder is transmitted. The overall code rate of a turbo code composed of two 1/2 rate RSC encoders is 1/3.

The Turbo encoder used in the proposed SDR transceiver shown in Figure 6 uses two constituent convolution encoders $E1$ and $E2$ in a parallel concatenated mode. Input bit string b_k of length N is encoded by $E1$ and $E2$. Equations (10) & (11) indicates the "parity bits" number which is transferred

$$P1 = \alpha N \tag{10}$$

$$\text{and } P2 = \left(1 - \alpha\right)N \tag{11}$$

Here α indicates "permeability rate". If α has a higher value, the convergence performances of the decoders of the proposed SDR transceiver is degraded by providing higher "Minimum Hamming Distance (MHD)". Equations (11) and (12) specify the fractional part of the codeword bits (θ_1 and θ_2)

$$\theta_1 = \frac{P1}{n} = 2\alpha R \tag{12}$$

$$\text{and } \theta_2 = \frac{P2}{n} = 2\left(-1\alpha\right)R \tag{13}$$

Here, the length of the codeword is denoted by n and R indicates the code rate of the proposed Turbo encoder used in the SDR transceiver system. The fractional data strings (θ_{q1} and θ_{q2}) are tackled by the component decoders of each code string are stated in the following equations (13) and (14)

$$\theta_{q1} = \frac{\alpha R}{1 + R} \tag{14}$$

$$\text{and } \theta_{q2} = \frac{\left(1 - \alpha\right)R}{1 + R} \tag{15}$$

'p' denotes the probability of error. For a given code rate the value of α has been selected.

Equation (16) denotes the overall code rate for the proposed Turbo encoder.

Figure 6. System Diagram for Proposed Turbo Encoder
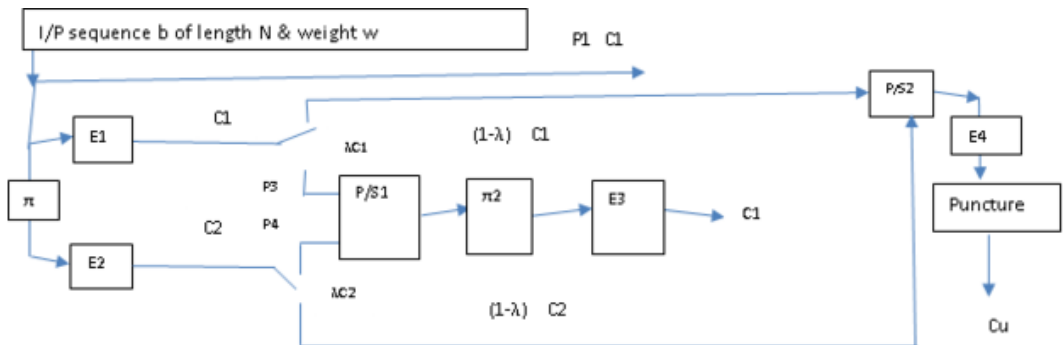
$$R = \frac{1}{1 + \alpha + 2(1 - \alpha)\text{Ál}} \tag{16}$$

The turbo encoder generator polynomial is given by Equation (17):

$$\begin{bmatrix} 1 & 1 & 1 \\ 1 & 0 & 1 \end{bmatrix} \tag{17}$$

The turbo encoder for the proposed SDR transceiver takes data at the input with a length of 1024 and provides output data of length 2052.

4.5 Turbo Decoding

To decode the bitstream on which turbo operation has been performed a turbo decoder is used. An estimate of the information sent can be found by solving posteriori log-likelihood ratios given by equations (18) and (19) (Sadjadpour 2000):

$$\Lambda_i^{(1)} = \log \frac{P[m_i = 1 \mid y^{(0)}, y^{(1)}, z^{(2)}]}{P[m_i = 0 \mid y^{(0)}, y^{(1)}, z^{(2)}]} \tag{18}$$

$$\tilde{\Lambda}_i^{(2)} = \log \frac{P[\widetilde{m_i} = 1 \mid \tilde{y}^{(0)}, y^{(1)}, \tilde{z}^{(2)}]}{P[\widetilde{m_i} = 0 \mid \tilde{y}^{(0)}, y^{(1)}, \tilde{z}^{(2)}]} \tag{19}$$

where

$y^{(0)}$ = information bits which are observed

$y^{(1)}$ = parity bits which are observed from the encoder on the top

$y^{(2)}$ = parity bits which are observed from the encoder on the bottom

$\tilde{y}^{(0)}$ = interleaved version of $y^{(0)}$

Λ = a posteriori log-likelihood ratio (LLR)

z = extrinsic information which is related to LLR by equations (20) and (21)

$$z_i^{(1)} = \Lambda_i^{(1)} - y_i^{(0)} - z_i^{(2)} \tag{20}$$

$$\tilde{z}_i^{(2)} = \tilde{\Lambda}_i^{(2)} - \tilde{y}_i^{(0)} - \tilde{z}_i^{(1)} \tag{21}$$

To solve the equations (18) to (19), the structure is shown in Figure 7 is used. Decoder1 determines solution to equation (18) and decoder2 determines solution to equation (19) (Sadjadpour 2000). Figure 7 represents the block diagram for the turbo decoder. The LLR is decoded by each decoder from the information received by it. The extrinsic information is then sent to the other decoders for further processing.

$$m_i = \begin{cases} 1 \, if \, \Lambda_i^{(2)} > 0 \\ 0 \, if \, \Lambda_i^{(2)} < 0 \end{cases} \tag{22}$$

Figure 7. Block diagram of the turbo decoder
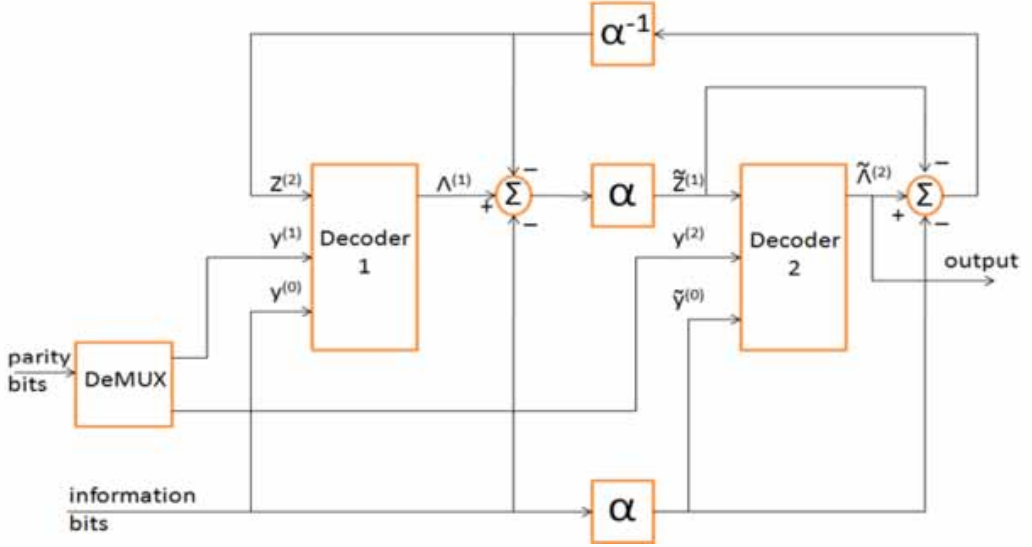
The a posteriori LLR's of (23) and (24) are computed by making use of the Max-Log-MAP algorithm (Sadjadpour 2000). While turbo codes offer extraordinary performance for bit error rates down to 10^{-5}, at SNR of around 10 dB, the performance for very small error rates is not impressive.

The maximum a posteriori (MAP) decoding algorithm is a technique that computes the LLR of each bit recursively based on the entire observed data block of length N as shown in equation (23) [2].

$$\Lambda_1\left(d_k\right) = Log \frac{\Pr(d_k = 1 \mid R_1^N)}{\Pr(d_k = 0 \mid R_1^N)} \tag{23}$$

$\Pr(d_k = 1 \mid R_1^N)$ is the a posteriori probability (APP) of the information at time k, represented by d_k, is equal to 1 given the entire received data. The received data sequence is represented by R_1^N = { $R_1, \ldots, R_{k\ldots}, R_N$ } where $R_k = \{ d_k^r \cdot y_k^n \}$ .The state of the encoder S_k is represented by equation (24)

$$S_k = (a_k, a_{k-1}, \ldots \ldots a_{k-v+1}) \tag{25}$$

Where a_k is the output of the first shift register in the Recursive Systematic Convolutional Code (RSC) encoder. The conditional joint probability $\Gamma_k^j\left(s\right)$ is defined as in equation (26)

$$\Gamma_k^j = \Pr\left(d_k = j, S_k\right) \tag{26}$$

The APP of d_k is equivalent to

$$\Pr d_k = j \mid R_1^N) = \sum_s \Gamma_k^j\left(s\right) j=0, 1 \tag{27}$$

$$\Lambda_1\left(d_k\right) = \log \frac{\sum_s \Gamma_k^1\left(s\right)}{\sum_s \Gamma_k^0\left(s\right)} \tag{28}$$

Equation (27) is written in terms of joint probabilities as

$$\Lambda_1\left(d_k\right) = \log \frac{\sum_s \sum_{s'} P_r\left(d_k = 1, s_k = s, S_{k-1} = s', R_1^N\right)}{\sum_s \sum_{s'} P_r\left(d_k = 1, s_k = s, S_{k-1} = s', R_1^N\right)} \tag{29}$$

$$\alpha_k\left(s\right) = p_r(s_k = s \mid R_1^k) \tag{30}$$

$$\beta_k\left(s\right) = \frac{\Pr(R_{k+1}^N \mid s_k = s)}{\Pr(R_{k+1}^N \mid R_1^k)} \tag{31}$$

$$\gamma_j\left(R_k, s', s\right) = \Pr(d_k = j, S_k = S, R_k \mid S_{k-1} = s') \tag{32}$$

The LLR in equation (xxxi) can be expressed as

$$\Lambda_1\left(d_k\right) = \log \frac{\sum_s \sum_{s'} \gamma_1\left(R_k, s', s\right)\alpha_{k-1}\left(s'\right)\beta_k\left(s\right)}{\sum_s \sum_{s'} \gamma_0\left(R_k, s', s\right)\alpha_{k-1}\left(s'\right)\beta_k\left(s\right)} \tag{33}$$

$\alpha_k\left(s\right)$ and $\beta_k\left(s\right)$ are computed by forward and backward recursions respectively based on $\gamma_j\left(R_k, s', s\right)$ as shown below in equation (34) & (35)

$$\alpha_k\left(s\right) = h_\alpha \sum_{s'} \sum_{j=0}^{1} \gamma_j\left(R_k, s', s\right)\alpha_{k-1}\left(s'\right) \tag{34}$$

$$\beta_k\left(s\right) = h_\beta \sum_{s'} \sum_{j=0}^{1} \gamma_j\left(R_{k+1}, s', s\right)\alpha_{k+1}\left(s'\right) \tag{35}$$

Where h_α and h_β are the normalization factors. The branch transition probability $\gamma_j\left(R_k, s', s\right)$ is given by equation (36)

$$\gamma_j\left(R_k, s', s\right) = \Pr\left(R_k \mid d_k = j, S_k = s, S_{k-1} = s'\right) \times \Pr\left(d_k = j \mid S_k = s, S_{k-1} = s'\right) \tag{36}$$

$$\beta_N\left(S_N\right) = \begin{cases} 1 & for\ S_N = 0 \\ 0 & otherwise \end{cases} \tag{37}$$

The decoder computes $\gamma_j(R_k, s', s)$ for j=0 and 1 upon receiving each d_k^r and its corresponding y_k^n. After that it computes and stores the value of α_k (s) $\forall$ s based on equation (36). After the data is collected, the backward recursion for β_k (s) is performed based on the equation (37). The LLR is then computed using the equation (31).

5. SDR TRANSCEIVER USING DECISION-BASED CARRIER TRACKING FOR M-QAM TECHNIQUE

The phase offset is considered to be denoted by θ. On this basis the offset of the received signal is given by equation (38)

$$\tilde{r}\left(nT\right) = r_{+}\left(nT\right)e^{-j\left(\omega_{e}nT+\theta\right)} \tag{38}$$

$$= \hat{c}_{n}e^{-j\theta} \tag{39}$$

where $c\hat{}_{n}$ = the output of a slicer. The baseband error at the receiver end is denoted by equation (40)

$$\tilde{e}\left(nT\right) = \hat{c}_{n} - \tilde{r}\left(nT\right) \tag{40}$$

The LMS update method is implemented to minimize a decision directed cost function, $J_{DD}\left(\theta\right)$ that consists of the mean squared baseband error

$$dJ_{DD}\left(\theta\right) = avg\left[\left\|\tilde{e}\left(nT\right)^{2}\right\|\right] \tag{41}$$

$$= avg\left[\tilde{e}\left(nT\right)\overline{\tilde{e}\left(nT\right)}\right] \tag{42}$$

By differentiating $JDD(\theta)$ concerning θ, we get

$$dJ_{DD}\left(\theta\right) = avg\left[\frac{d\left[\tilde{e}\left(nT\right)\overline{\tilde{e}\left(nT\right)}\right]}{d\theta}\right] \tag{43}$$

$$= 2avg\left[\Re e\left\{\overline{\tilde{e}\left(nT\right)}\frac{\mathrm{d}e\left(nT\right)}{\mathrm{d}\theta}\right\}\right] \tag{44}$$

Where

$$\frac{\mathrm{d}\tilde{e}\left(nT\right)}{\mathrm{d}\theta} = \frac{d}{\mathrm{d}\theta}\left[\hat{c}_{n} - \tilde{r}\left(nT\right)\right] = -\frac{\mathrm{d}\tilde{r}\left(nT\right)}{\mathrm{d}\theta} \tag{45}$$

And

$$\frac{\mathrm{d}\tilde{r}\left(nT\right)}{\mathrm{d}\theta} = -j\hat{c}_{n}\mathrm{e}^{-j\theta} = j\tilde{r}\left(nT\right) \tag{46}$$

$$\frac{dJ_{DD}\left(\theta\right)}{d\theta} = 2avg\left[\Re e\left\{\overline{\tilde{e}\left(nT\right)}j\tilde{r}\left(nT\right)\right\}\right] \tag{47}$$

$$= -2avg\left[\Im m\left\{\overline{\tilde{e}\left(nT\right)}\tilde{r}\left(nT\right)\right\}\right] \tag{48}$$

$$= -2avg\left[\Im m\left\{\overline{\hat{c}_{n}}\tilde{r}\left(nT\right)\right\}\right] \tag{49}$$

where $\Im m$ [.] = imaginary part of the complex value [.]. In the polar form, we get

$$\Im m\left\{\overline{\hat{c}_{n}}\tilde{r}\left(nT\right)\right\} = \Im m\left\{R_{e}e^{j\beta_{e}}R_{r}e^{j\beta_{r}}\right\} \tag{50}$$

$$= R_c R_r \sin\left(\beta_r - \beta_c\right) \tag{51}$$

Thus

$$\sin\left(\beta_r - \beta_c\right) = \frac{\Im m\left\{\hat{c}_n \overline{\tilde{r}\left(nT\right)}\right\}}{R_c R_r} \tag{52}$$

To determine the phase update the phase error is multiplied by a small scale factor as shown in equation (53):

$$\Delta\phi\left(n\right);\ \Delta\theta\left(n\right) = \frac{\Im m\left\{\overline{\tilde{e}\left(nT\right)}\,\tilde{r}\left(nT\right)\right\}}{\left|c_n\right|^2} \tag{53}$$

When both phase and frequency tracking are considered, the carrier phase of the receiver becomes

$$\phi\left(n+1\right) = \phi\left(n\right) + \Delta\phi\left(n\right) \tag{54}$$

Phase update $\Delta\phi\left(n\right)$ is denoted by

$$\Delta\phi\left(n\right) = k\Delta\theta\left(n\right) + \psi\left(n\right) \tag{55}$$

where ψ(n) is the contribution of frequency tracking and can be further expressed by equation (56):

$$\psi\left(n\right) = \psi\left(n-1\right) + k_2\Delta\theta\left(n\right) \tag{56}$$

The scale factors k_1 and k_2 are assumed to be small here and usually $k_1/k_2^3 100$ required for phase convergence. Figure 8 depicts the frequency and carrier phase tracking based on decision used in the proposed SDR transceiver system for exact recovery of the data transmitted at the receiver end.

Figure 8. Decision-based carrier phase and frequency tracking
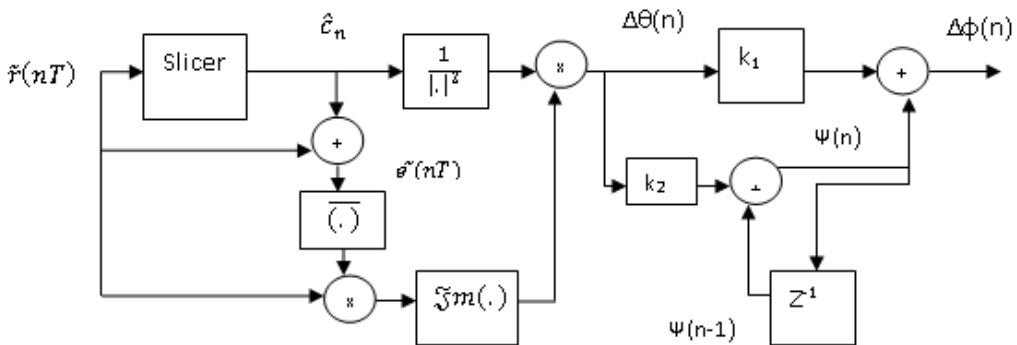
It is observed that the received signal changes on the introduction of noise in the channel. Figure 9 shows the VI for Frequency and Phase Tracking. According to the literature survey done (Kim, Kehtarnavaz, and Torlak 2006)(Sadiku and Akujuobi 2004),(Noseworthy 2007)(Mitola 1999)(Ramacher 2007)(Baines and Pulley 2003)(Cummings and Haruyama 1999)(Hatai and Chakrabarti 2009)(Ibrahim, Alias, and Ahmad 2013), it has been observed that the real-time testing of the Decision-Based Carrier Tracking for SDR supporting M-ary modulation schemes has not been done. A few instances in the literature suggests that the SDR has been simulated separately for FSK, PSK, QAM (Oza et al. 2010)(Kim et al. 2006)(Özyurt, Serdar, Oˇguz Kucur 2007) and other digital modulation techniques. The proposed SDR transceiver supports real-time secured transmission and reception of data with the flexibility of changing the protocols and using Forward Error-Correcting codes (FEC) using the M-ary digital modulation technique QAM. Different pulse shaping filters such as Root-raised cosine and Raised cosine filter has been used. A fully reconfigurable digital transceiver has been proposed, simulated and tested using NI USRP-2922.

5.1 Front END Implementation of the proposed
M-QAM, SDR Transmitter USING USRP

The front end implementation of the proposed SDR transmitter includes the generation of the IQ waveform from the USRP module. The acquired waveform is fed to the shift register for pipelining. Then the acquired IQ signal is sampled to multiples of the expected symbol rate. The signal is then modulated according to the type of data to be transmitted. The matching filter adds a transient to the modulated signal and it is then Transmitted. The signal and check for the constellation graph display niUSRP Configure Signal VI is done to verify the parameters of the transmitted signal.

Figure 10 show the Front panel for the Transmitter section of the SDR system using LabVIEW. Tx Parameter in Figure 10 are used to select Transmitter parameters. USRP IP address field helps to select the IP address of the transmitter device. Tx 'IQ' Sampling Rate [s/sec] is used to set the Sampling rate to 500k for text and binary data and < 2M for the image. Tx Frequency field is used to set the Frequency for the transmission (2.5GHz). (User has the option to use any frequency from 400MHz to 4.4GHz for USRP 2922). Tx Gain (dB) is used to enter Tx Gain at the transmitter end (12 dB – 31 dB). Tx Antenna is used to select the Tx Antenna as Tx1.

To transmit the data in real-time the tab, 'specify message' tab is selected in the transmitter front panel as shown in Figure 10. There are three options for transmitting such as the Random data, Text and image. The number of bits to be transmitted is indicated by the transmitted bits. The

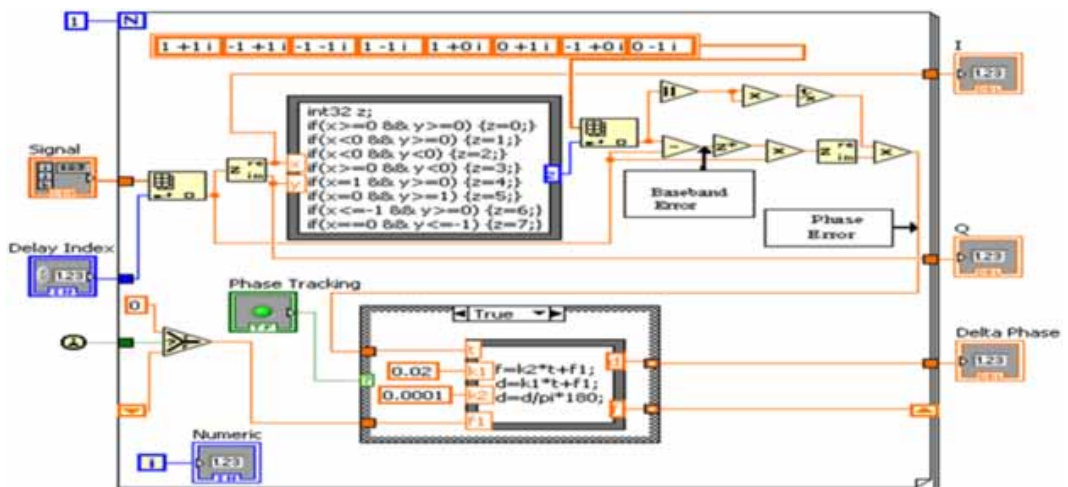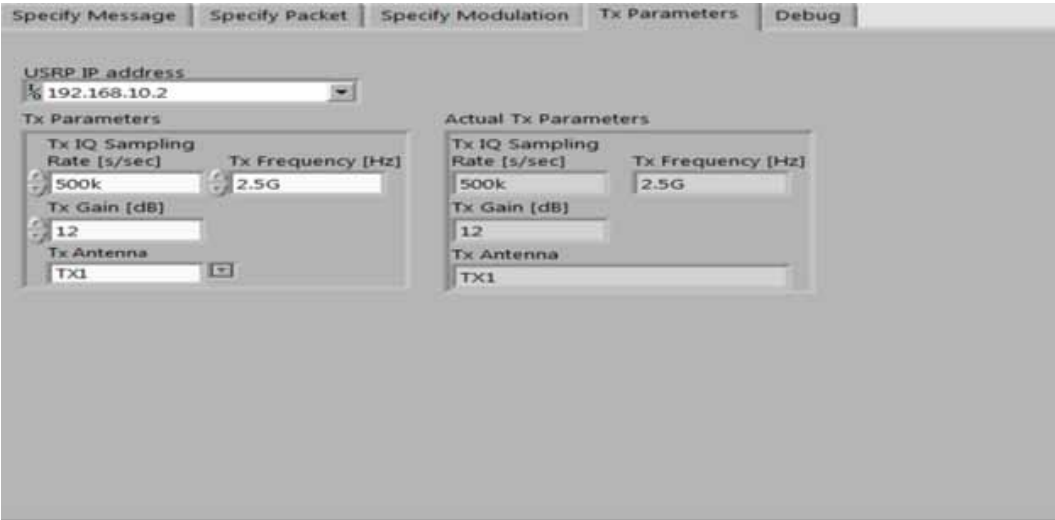**Figure 9. Phase and Frequency Tracking VI**

Figure 10. Front Panel of Transmitter

data to be sent is encoded using the Tubo Coding/Convolution Coding by selecting from the type of encoding button. The proposed SDR transceiver supports the transmission of binary data, text or image respectively as shown by Figure 11.

Figure 11 depicts how the proposed system is used for transmitting the Text and similarly, the data to be sent is encoded using the Tubo Coding/Convolution Coding by selecting from the type of encoding button. The modulation tab is used to set the type of M-ary modulation scheme i.e. QAM. Specify packet tab shown in Figure 12 is used to set the characteristics of the real-time data to be transmitted from the transmitter end.

5.2 Implementation of the proposed M-QAM, SDR Receiver USING USRP

The front end implementation of the proposed M-QAM SDR receiver includes the acquiring of the IQ waveform from the USRP module. The acquired waveform is fed to the shift register for pipelining.

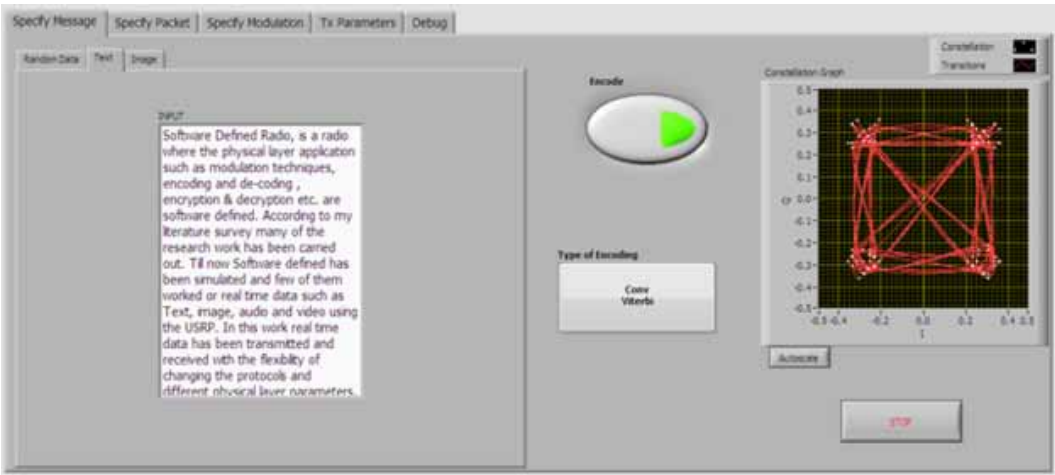**Figure 11. Specify Message/Text Window**

Figure 12. Specify Packet for Transmission

Then the acquired IQ signal is Resampled to multiples of the expected symbol rate. The signal is then demodulated according to the type of data to be transmitted. The matching filter then truncates a transient from the demodulated signal at the receiver end. The signal and check for the constellation graph display niUSRP Configure Signal VI is done to verify the parameters of the received signal using niUSRP Configure Signal VI. The waveform acquisition in an Rx session is initiated by the initiate start button. The Rx session has to be initiated before the transmission of the data starts from the transmitter side to retrieve waveform data completely. When data is provided to the transmitter the transmission is initiated using the niUSRP Write Tx Data VI. The front panel of the Receiver is shown in Figure 13. In this panel, the Rx Parameter window is selected to specify the IP address for the receiver side USRP and configure the Rx parameters and the Acquisition Duration time at the receiver end in (sec).

Rx 'IQ' Sampling Rate [s/sec] on the receiver side as shown in Figure 13 is used to set the Sampling rate to 500k. Rx Frequency (Hz) field is used to set the Frequency to 2.5GHz. Rx Gain is measured in (dB) and a value similar to the transmitter is entered here i.e. 12dB. The Rx Antenna field is used to select the Rx Antenna for reception through the USRP. Rx1 is selected for the same. Acquisition Duration measured in (sec) is set according to the type of file to be received. Different parameters such as the constellation diagram, eye diagram and BER vs. E_b/N_o ratio with respective received data are analysed and represented for analysis as shown in Figure 14.

Figure 14 shows the different Output Parameters at the receiver end. The 'Constellation Graph' indicates the constellation Graph of the Received bits concerning data. The 'Eye Diagram' is plotted on a chart that indicates the waveform segments for the eye diagram display of the Received bits concerning data. Display 'I/Q' specifies whether to generate 'I' data or 'Q' data to the eye diagram. Eye length input in the VI gives the number of symbol periods on the horizontal scale of the eye diagram. Figure 15 shows the experimental setup for the proposed SDR system using NI-USRP 2922. Figure 16 (a, b, c, d, e, f, g) depicts the constellation diagram, Eye diagram, BER vs. E_b/N_o Output curve for Convolution Coding using 4-QAM, 8-QAM, 16-QAM, 32-QAM, 64-QAM, 128-QAM, 256-QAM for the received binary data, text and image.

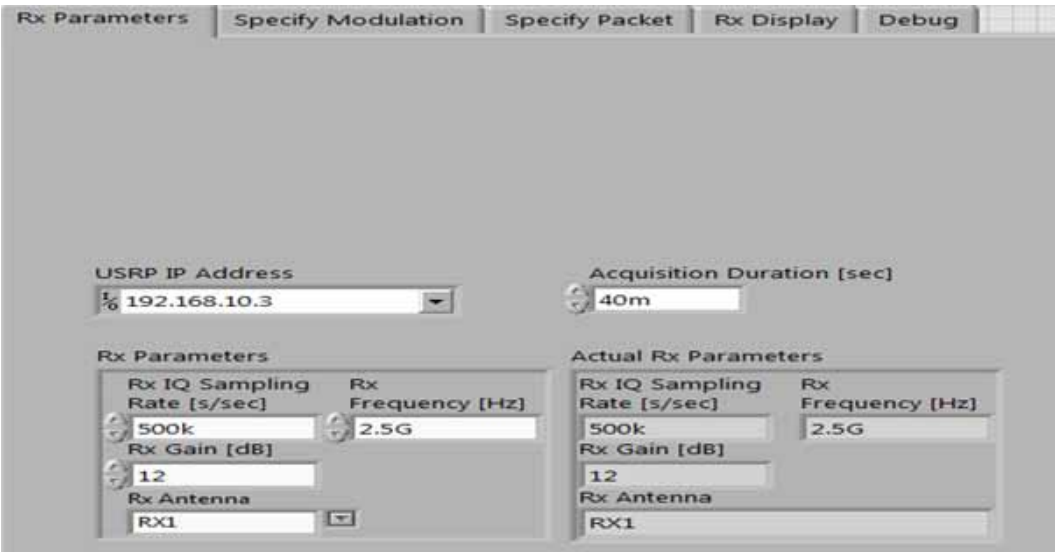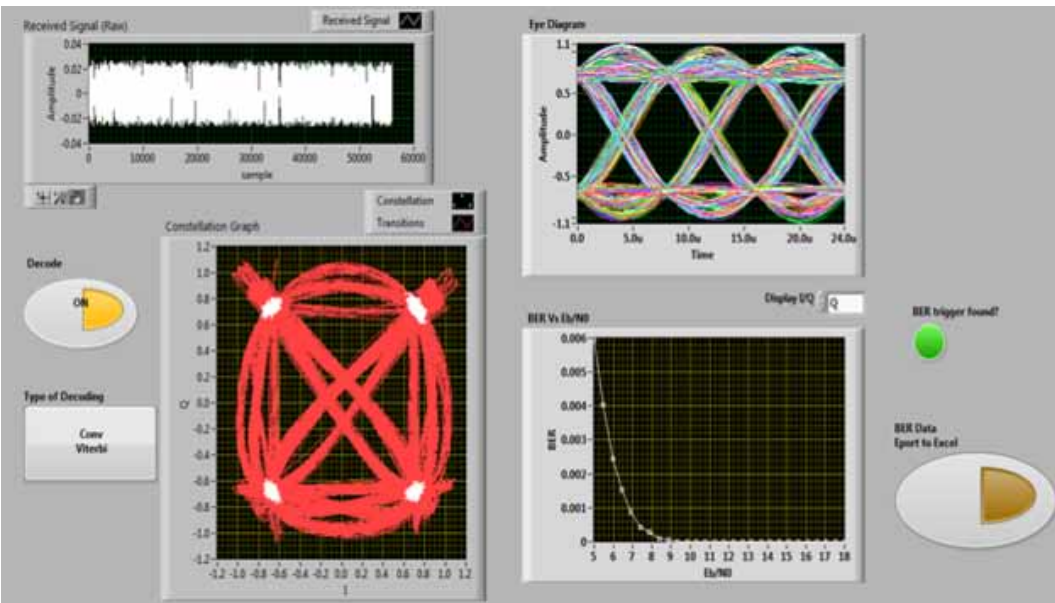**Figure 13. Front Panel of USRP Receiver/ Rx Parameter**

Figure 14. Output Parameters

6. ANALYSIS OF RESULTS OBTAINED

The analysis of the M-QAM signal is shown in Figure 16. The analysis of the results has been done based on the constellation diagram, Eye diagram and the BER vs. E_b/N_o Output curve. Figure 16 (a, b, c, d, e, f, g) represents the analysed data by the proposed SDR transceiver. The decision points are highlighted through the constellation plot which helps to analyze phase errors, as well as amplitude

Figure 15. Experimental Setup of the Proposed SDR system using NI-USRP 2922
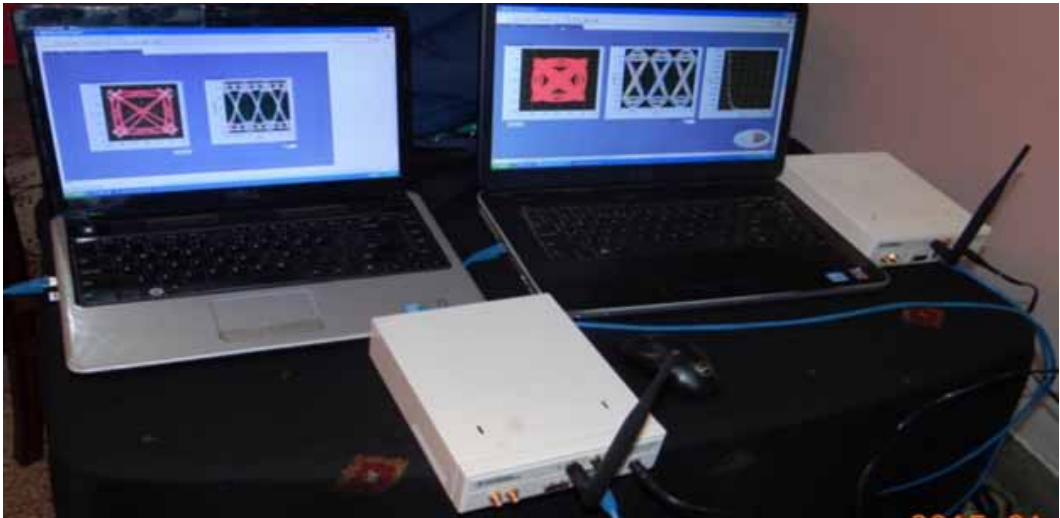
errors at these decision points. The constellation diagram also helps to analyse many impairments in the received signal.

The data to be transmitted is first encoded by using either turbo coding or convolution coding and then modulated by using QAM and transmitted over the channel through USRP. In the output of the turbo coding using the QAM modulation scheme, it is observed that:

- As the M-ary transmission is increased using QAM modulation, the noise in real-time increases by 0.4 dB.
- With the increase in several phases, the distortion tends to be under the limit of 0.1 Hz.
- The SNR tends to reduce from 0.6 to zero with an increase in many phases.
- As the number of phase increases, the deviation of the signal from the true periodicity increases from 0.1s to 1s.

Table 3 shows the different parameters used while using Turbo coding algorithm for the M-QAM modulation technique. The Table 3 helps us to analyze how the distortion in the signal is increasing as we increase the higher-order modulation of QAM. Figure 17 and Figure 18 represent the output of the proposed SDR system in terms of transmitted Image using Convolution Coding/ Viterbi Decoding and Turbo Coding and decoding respectively.

The image sent from the transmitter gets corrupted by noise in the channel which is air and then is downloaded by the designated receiver which has the key to decode the respective image. Hence the system is secure and also provides better BER concerning any other systems. The biggest advantage of the proposed design is that it is meant to work for real-time input and hence the output obtained is for real-world use.

From Figure 17 and Figure 18 it is pretty much clear that for higher-order QAM the output gets distorted and posses higher errors while using convolution coding. When the same transfer is made using Turbo coding the time taken to receive the image is a bit more but the quality of the image received is much better than that for convolution coding. Table 4 highlights the features of the proposed SDR Transceiver System Using NI USRP for Real-time data transfers and it can be seen that Turbo coding performs much better than convolution coding. Through the table, it can be seen that the average SNR value for the M-QAM technique is (>10.2812dB) for Turbo coding with the

Figure 16. Different parameters (Constellation diagram, Eye diagram, BER vs. E$_b$/N$_o$ ratio) for the analyses of the results using Convolution Coding for different M-ary QAM: a) 4-Bit, b) 8 -Bit, c) 16 -Bit, d) 32 -Bit, e) 64 -Bit, f) 128 -Bit, g) 256 -Bit
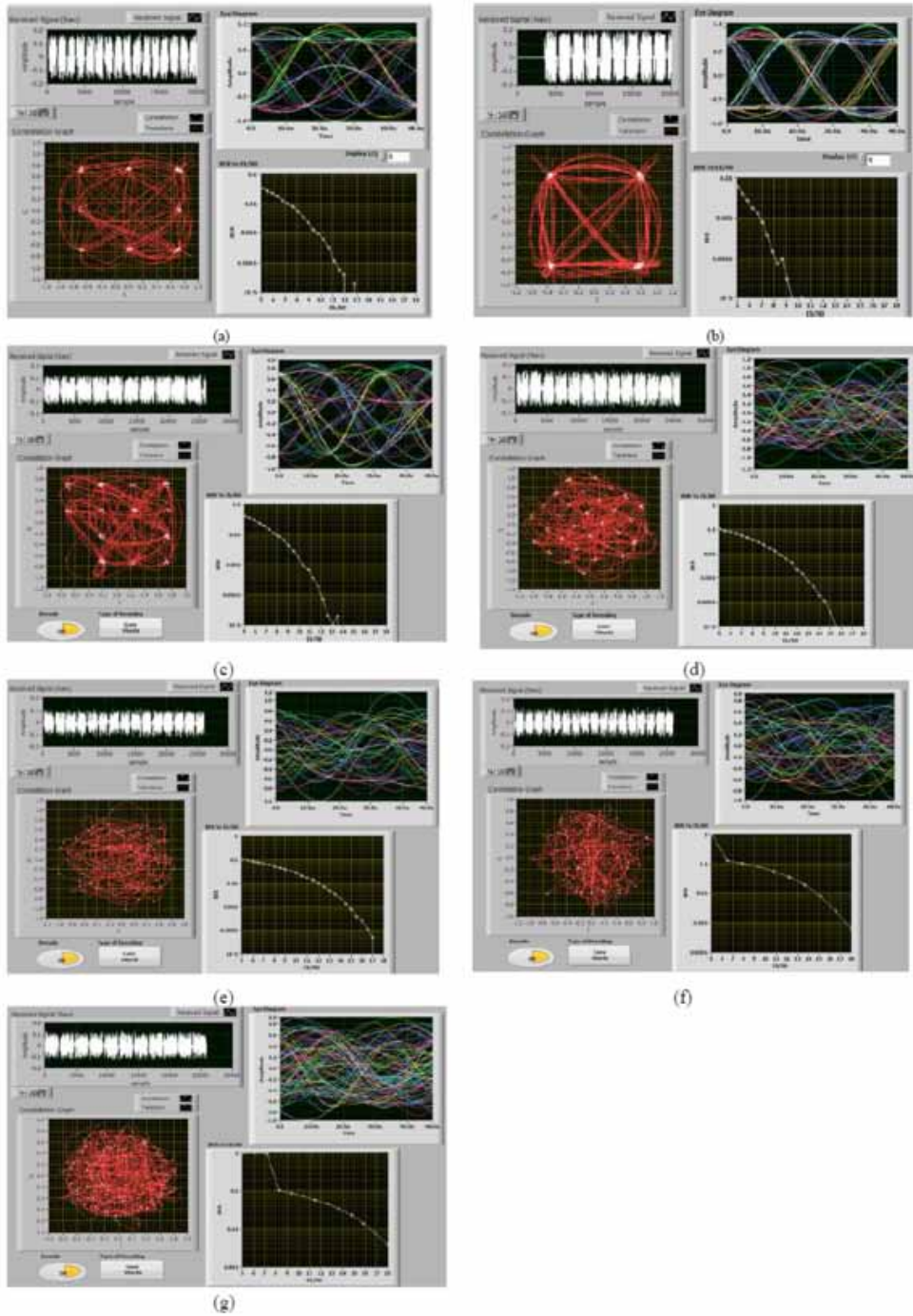
Table 3. Parameters for QAM Modulation using Turbo Coding for different M-ary QAM

Parameter\ Signals (Turbo Coding)	4	8	16	32	64	128	256
Additive noise (Peak to Peak)	1.4	1.8	2.2	2.2	2.2	2.2	2.2
Distortion due to addition of noise (Overshoot/Undershoot) (Hz)	0.1	0.2	0.2	0.4	0.35	0.4	0.1
SNR (dB)	0.6	0.4	0.2	0.05	0.05	0.05	0
Deviation from true periodicity (s)	0.1	0.1	0.2	0.4	0.6	0.9	1

Figure 17. Encoded and Decoded output Image obtained for QAM Modulation and Convolution Coding using different M-ary QAM: a) 4-Bit, b) 8-Bit, c) 16 -Bit, d) 32-Bit, e) 64-Bit, f) 128 -Bit, g) 256-Bit
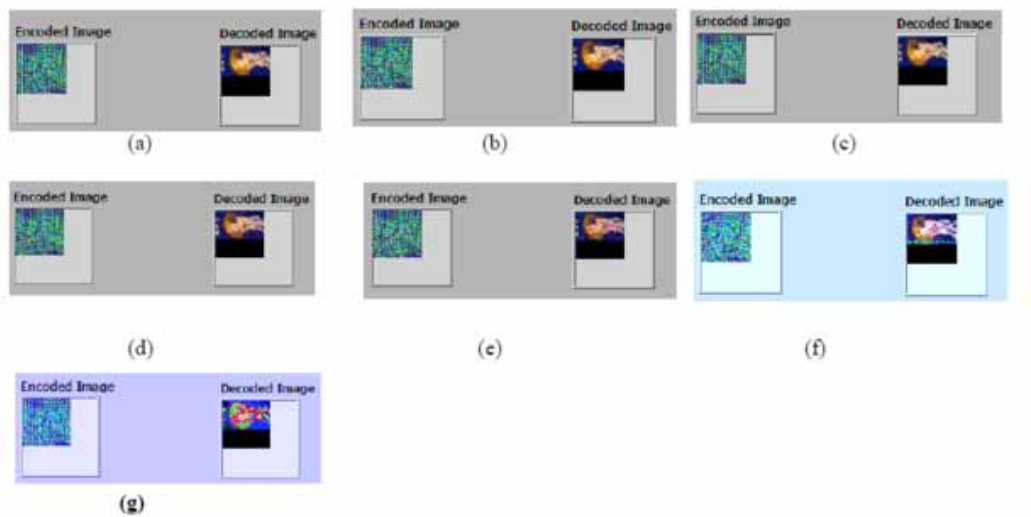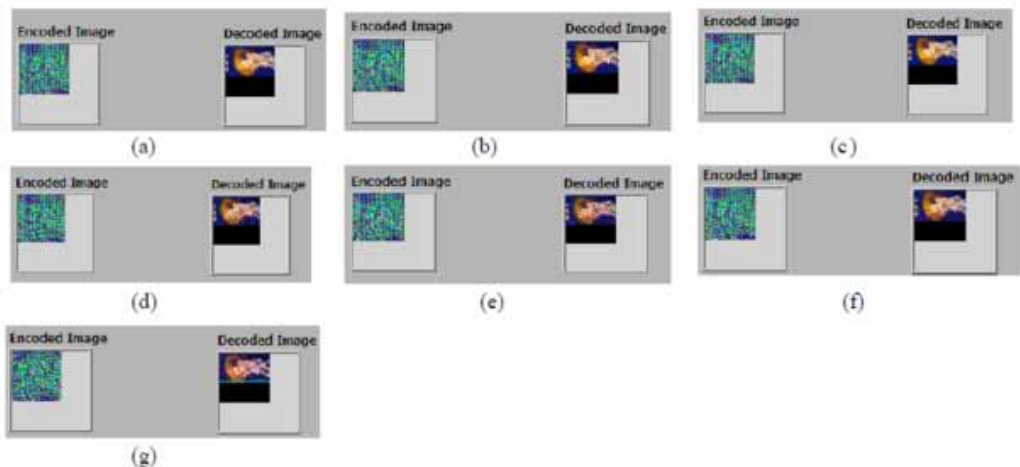

Figure 18. Encoded and Decoded output Image obtained by using QAM Modulation and Turbo Coding using: a) 4-Bit, b) 8-Bit, c) 16-Bit, d) 32-Bit, e) 64-Bit, f) 128-Bit, g) 256-Bit

average BER vs. (E_b/N_o) as 14.3 whereas under similar conditions the average SNR value for M-QAM technique using Convolution coding is (>10.2812dB) with the average BER vs. (E_b/N_o) as 14.5. It is concluded that under similar conditions the performance of Turbo coding comes out to be much better as compared with that of the Convolution Coding.

Table 5 represents the performance comparison between the proposed SDR Transceiver system using NI USRP for real-time data transfer for 4-bit QAM and state-of-the-art SDRs. Compared to SDRs presented in the literature, the proposed SDR Transceiver system closely adheres to the SDR concept by which most of the transceiver operation and radio hardware is configured through software programming in order to approximate a complete software-controlled operation based on a fully digital hardware architecture using NI USRP.

7. GRAPHICAL REPRESENTATION OF THE RESULTS OBTAINED

The graphical representation of the obtained results is shown by Figures 19, 20, 21, and 22. The chart comprises the BER vs. Eb/No curve for QAM based SDR Transceiver using Convolution coding/ Viterbi Decoding and Turbo coding and decoding using raised cosine filter and root raised cosine filter.

With the help of the results represented by Figure 19, 20, 21, and 22 it is proved that the lower-order M-QAM technique gives a better BER Turbo coding and decoding than that of the Convolution coding/Viterbi Decoding. It is also seen that as we move to higher-order M-QAM techniques the noise in the output is more and the BER value is not good, hence it is recommended that for the existing systems a lower order M-QAM should be used for the transmission.

8. CONCLUSION

The proposed model provides enhanced flexibility for the implementation of the SDR system as the proposed system has no constraints of the packet size, data rates, and processing speed and the same has been tested on standard hardware the USRP-2922. The proposed system is tested extensively in real-time conditions by transferring the data in different forms such as binary codes or text and image. Based on the results obtained in the present study, it can be seen that the M-QAM shows a better

Table 4. The features of the proposed SDR Transceiver System Using NI-USRP for Real-time data transfers

Ref. Features	Proposed SDR Transceiver system (Using NI USRP for Real-time data transfer for 4-bit QAM)	
	Convolution Coding	Convolution Coding
Bandwidth	10 kHz-4.4 GHz	10kHz-4.4 GHz
SNR	>14.6087dB	>10.2812dB
Data Rate(Mbps)	50	45
Application	Wide Application	Wide Application
BER vs. (Eb/No)	14.5	14.3
Reliability	Highly Reliable	Highly Reliable
Hardware Complexity	Easy to Modify	Easy to Modify
Hardware Cost	Very Low	Very Low
Implementation on FPGA	Very Easy Implementation	Very Easy Implementation
Modulation	M-QAM	M-QAM
Coding Techniques	Convolution, Turbo Coding	Convolution, Turbo Coding

Table 5. Performance comparison between the proposed SDR Transceiver system using NI USRP for real-time data transfer for 4-bit QAM and state-of-the-art SDRs

Ref. Features	Existing SDR Systems								Proposed SDR Systems
	(Roth, Manjikian, and Sudharsanan 2009)	(Zou, Mikhemar, and Sayed 2009)	(Martinek, Al-Wohaishi, and Zidek 2010)	(Oza et al. 2010)	(Scotti et al. 2015)	(Kwag et al. 2015)	(Marimuthu, Bialkowski, and Abbosh 2016)	(Fepeussi et al. 2019)	
Bandwidth	-	1GHz range	20 MHz	2.5GHz	2.53GHz	2.5GHz	2.0GHz	5GHz	10kHz- 10 GHz
SNR	-	27.5 dB	-	20dB	25dB	20dB	15dB	12dB	>10.2812dB
Data Rate(Mbps)	-		13	25	30	35		40	50
Application	-	-	Real measurement of error rate	Video. Image	Cognitive sensing	Wave Sensing	Near-Field Biomedical Imaging	Indoor Positioning	Wide Applications Real-Time/ Cognitive measurements
E_b/N_0 dB	2.7dB	-	28 dB(32-PSK);21 dB(64-QAM)	35 dB	-	-	-	-	14.3
BER	10^{-1}	10^{-4}	10^{-4}	10^{-4}	10^{-5}	10^{-5}	10^{-4}	10^{-5}	10^{-5}
Reliability	Less	-	-	High	High	High	High	High	Highly Reliable
Hardware Complexity	Complex	Less Complex	Complex	Low Bandwidth	Complex	Less Complex	Less Complex	Less Complex	Easy to Modify
Hardware Cost	High	Low	High	Low	Low	Low	Low	Low	Very Low
Hardware	-	-	-	-	PXIe-5451 AWG	-	Blade RF SDR (GNU Radio)	AD9361 SDR	USRP-2922
Modulation	QPSK	QPSK	M-QAM, M-PSK	FSK, QPSK	FMCW	-	SFCW	S-MFCW	Convolution, Turbo Coding
Coding Techniques	-	-	-	-	-	-	-	-	FEC Coding

Figure 19. BER vs. Eb/No curve for QAM Transceiver using Convolution coding with raised cosine filter
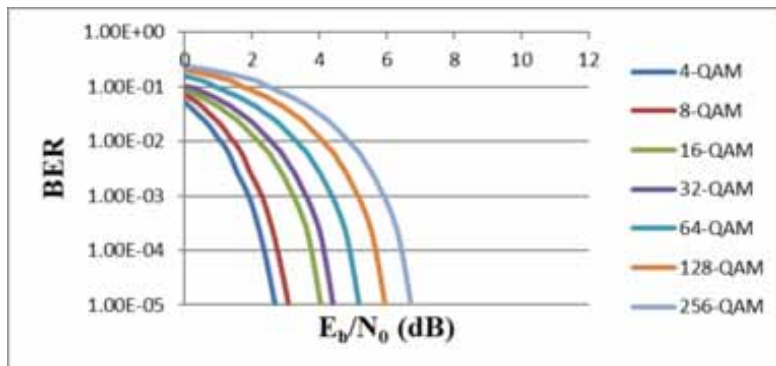
performance for lower modulation order whereas the out gets inferior as we move to a higher order of 'M'. Therefore, it can be concluded that the lossless reproduction of the data in the form of (binary bits, text or image) can be achieved at the receiver end with the use of lower order of modulation. The use of FEC codes makes the system more secure and future-ready. Analysis of experimental results shows that, compared to a conventional transceiver with similar functions, the proposed

Figure 20. BER vs. Eb/No curve for QAM Transceiver using Convolution coding with root raised cosine filter
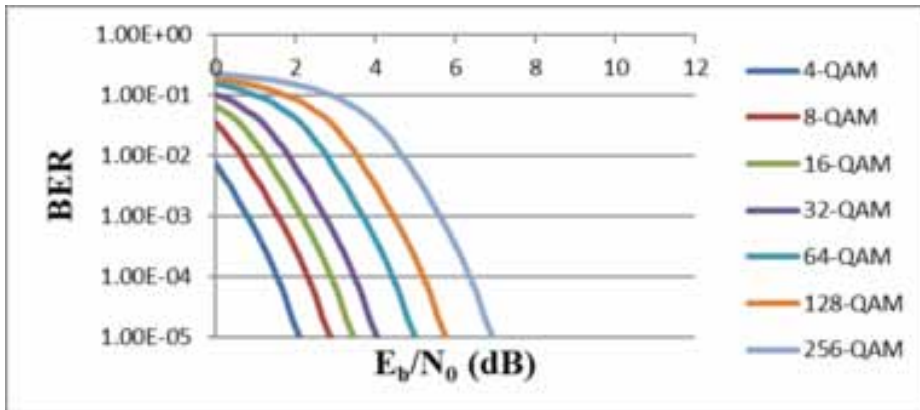

Figure 21. BER vs. Eb/No curve for QAM Transceiver using Turbo coding with raised cosine filter
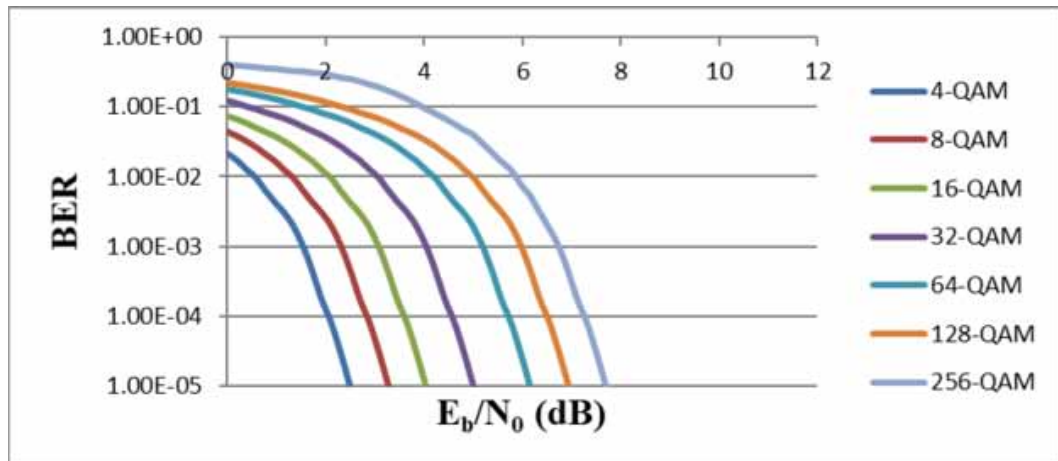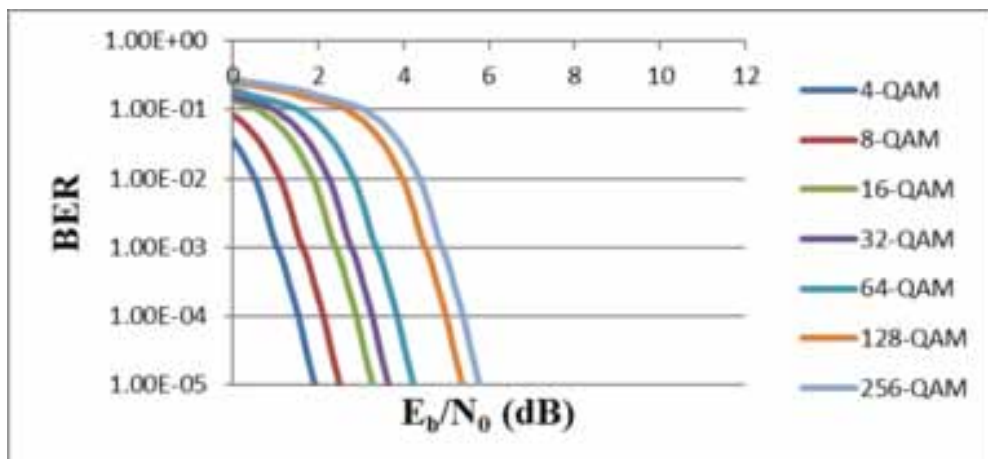

Figure 22. BER vs. Eb/No curve for QAM Transceiver using Turbo coding with raised cosine filter

SDR transceiver system achieves a very low BER of the order of 10^{-5} with SNR of 14.67 dB using convolution coding and an SNR of 10.28 dB for turbo coding respectively for real-time transfer of data at the rate of 20Mbps. At BER of 10^{-5} and data rate of 20Mbps the BER vs. (Eb/No) achieved was around 14.3. The proposed model provides enhanced flexibility for the implementation of the SDR system as the proposed system has no constraints of the packet size, data rates, and processing speed and the same has been tested on standard hardware the USRP-2922. The proposed SDR transceiver system is tested extensively in real-time conditions by transferring the data in different forms such as binary codes or text and image. Based on the results obtained in the present study, it can be seen that the M-QAM shows a better performance for lower modulation order whereas the out gets inferior as we move to a higher order of 'M'. Therefore, it can be concluded that the lossless reproduction of the data in the form of (binary bits, text or image) can be achieved at the receiver end with the use of lower order of modulation. The use of FEC codes makes the system more secure and future-ready. The proposed SDR transceiver system uses decision-based carrier tracking which ensures that phase tracking routine, the phase error, affected by the initial phase and frequency difference, is minimized and the received signal becomes a perfect reproduction of the transmitted signal except for the time delay. As the progress of the tracking operation takes place the constellation of the samples in the I-Q plane becomes that of the ideal reference. The proposed SDR transceiver system shows that the lower-order M-QAM technique gives a better BER for Turbo coding and decoding than that of the Convolution coding/Viterbi Decoding.

REFERENCES

Adachi, F., & David Parsons, J. (1989). Error Rate Performance of Digital FM Mobile Radio with Postdetection Diversity. *IEEE Transactions on Communications*, *37*(3), 200–210. doi:10.1109/26.20093

Baines, R., & Pulley, D. (2003). A Total Cost Approach to Evaluating Different Reconfigurable Architectures for Baseband Processing in Wireless Receivers. *IEEE Communications Magazine*, *41*(1), 105–113. doi:10.1109/MCOM.2003.1166666

Bhanubhai, P. S., Shajan, M. G., & Dalal, U. D. (2012). Performance of Turbo Encoder and Turbo Decoder for LTE. *International Journal of Engineering and Innovative Technology*, *2*(6), 125–128.

Bloessl, B., Segata, M., Sommer, C., & Dressler, F. (2018). Performance Assessment of IEEE 802.11p with an Open Source SDR-Based Prototype. *IEEE Transactions on Mobile Computing*, *17*(5), 1162–1175. doi:10.1109/TMC.2017.2751474

Bloessl, B., Segata, M., Sommer, C., & Dressler, F. (2018). Performance Assessment of IEEE 802.11p with an Open Source SDR-Based Prototype. *IEEE Transactions on Mobile Computing*, *17*(5), 1162–1175. doi:doi:10.1109/TMC.2017.2751474

Borle, K. M., Zhao, Y., & Chen, B. (2014). A Software Radio Design for Communications in Uncoordinated Networks. *IEEE 15th International Workshop on Signal Processing Advances in Wireless Communications (SPAWC)* 254–58. doi:10.1109/SPAWC.2014.6941584

Cummings, M., & Haruyama, S. (1999). Fpga in the Software Radio. *IEEE Communications Magazine*, *37*(2), 108–112. doi:10.1109/35.747258

Fellenberg, C., & Rohling, H. (2009). Quadrature Amplitude Modulation for Differential Space-Time Block Codes. *Wireless Personal Communications*, *50*(2), 247–255. doi:10.1007/s11277-008-9587-x

Fepeussi, T. V., Testi, N., Xu, Y., & Jin, Y. (2019). High-Accuracy Narrowband Software-Defined Radar Using Successive Multiple-Frequency Continuous-Wave Modulation for Sensing Applications. *IEEE Transactions on Microwave Theory and Techniques*, *67*(9), 3917–3927. doi:10.1109/TMTT.2019.2910056

Fepeussi, T. V., Testi, N., Xu, Y., & Jin, Y. (2019). High-Accuracy Narrowband Software-Defined Radar Using Successive Multiple-Frequency Continuous-Wave Modulation for Sensing Applications. *IEEE Transactions on Microwave Theory and Techniques*, *67*(9), 3917–3927. doi: doi:10.1109/tmtt.2019.2910056

Fepeussi, T. V., Testi, N., Xu, Y., & Jin, Y. (2019). High-Accuracy Narrowband Software-Defined Radar Using Successive Multiple-Frequency Continuous-Wave Modulation for Sensing Applications. *IEEE Transactions on Microwave Theory and Techniques*, *67*(9), 3917–3927. doi: doi:10.1109/tmtt.2019.2910056

Fleming, C. (2002). A Tutorial on Convolutional Coding with Viterbi Decoding. *Spectrum Applications,* 1–28.

Gandhiraj, R., & Soman, K. P. (2014). Modern Analog and Digital Communication Systems Development Using GNU Radio with USRP. *Telecommunication Systems*, *56*(3), 367–381. doi:10.1007/s11235-013-9850-7

Hatai, I., & Chakrabarti, I. (2009). FPGA Implementation of a Digital FM Modem for SDR Architecture. *Computers and Devices for Communication, 2009, (pp. 0-3).*

Ibrahim, S. A., Alias, M. Y., & Ahmad, N. N. (2013). Performance of Adaptive Modulation Scheme for Adaptive Minimum Symbol Error Rate Beamforming Receiver. *Wireless Personal Communications*, *71*(2), 873–886. doi:10.1007/s11277-012-0849-2

Javornik, T., Mohorčič, M., Švigelj, A., Ozimek, I., & Kandus, G. (2005). Adaptive Coding and Modulation for Mobile Wireless Access via High Altitude Platforms. *Wireless Personal Communications*, *32*(3–4), 301–317. doi:10.1007/s11277-005-0747-y

Kim, N., Kehtarnavaz, N., & Torlak, M. (2006). LabVIEW-Based Software-Defined Radio: 4-QAM Modem. *Journal of Systemics, Cybernetics And Informatics*, *4*(3), 54–61.

Kumar, N., Rawat, M., & Rawat, K. (2020). Software-Defined Radio Transceiver Design Using FPGA-Based System-on-Chip Embedded Platform with Adaptive Digital Predistortion. *IEEE Access: Practical Innovations, Open Solutions*, *8*, 214882–214893. doi:10.1109/ACCESS.2020.3041463

Kumar, N., Rawat, M., & Rawat, K. (2020). Software-Defined Radio Transceiver Design Using FPGA-Based System-on-Chip Embedded Platform with Adaptive Digital Predistortion. *IEEE Access: Practical Innovations, Open Solutions*, *8*, 214882–214893. doi:10.1109/ACCESS.2020.3041463

Kumar, N., Rawat, M., & Rawat, K. (2020). Software-Defined Radio Transceiver Design Using FPGA-Based System-on-Chip Embedded Platform with Adaptive Digital Predistortion. *IEEE Access: Practical Innovations, Open Solutions*, *8*, 214882–214893. doi: doi:10.1109/ACCESS.2020.3041463

Kunisawa, Y., Kamisaka, D., Watanabe, S., & Takeuchi, Y. (2007). An Initial Acquisition Scheme for Software Defined CDMA2000 1xEV-DO Radio Terminal. *IEEE International Symposium on Personal, Indoor and Mobile Radio Communications, PIMRC*. IEEE. doi:10.1109/PIMRC.2007.4394561

Kwag, Y. K., & Jung, J. S. (2015). Multi-Band Multi-Mode SDR Radar Platform. *Proceedings of the 2015 IEEE 5th Asia-Pacific Conference on Synthetic Aperture Radar, APSAR 2015,* (pp. 46–49). IEEE. doi:10.1109/APSAR.2015.7306151

Kwag, Y. K., Jung, J. S., Woo, I. S., & Park, M. S. (2015). Multi-band multi-mode SDR radar platform. *Proc. 2015 IEEE 5th Asia-Pacific Conf. Synth. Aperture Radar, APSAR 2015*, (pp. 46–49). IEEE. doi: 10.1109/APSAR.2015.7306151

Liu, C. (2006). Design and Implementation of Software Radio Based Signal Generator Using LabVIEW. *1st International Symposium on Systems and Control in Aerospace and Astronautics, ISSCAA 2006* (pp. 1259–62).

Marimuthu, J., Bialkowski, K. S., & Abbosh, A. M. (2016). Software-Defined Radar for Medical Imaging. *IEEE Transactions on Microwave Theory and Techniques*, *64*(2), 643–652. doi:10.1109/TMTT.2015.2511013

Marimuthu, J., Bialkowski, K. S., & Abbosh, A. M. (2016). Software-defined radar for medical imaging. *IEEE Transactions on Microwave Theory and Techniques*, *64*(2), 643–652. doi: doi:10.1109/TMTT.2015.2511013

Marriwala, Nikhil, O. P. Sahu, & Vohra, A. (2013). 8-QAM Software Defined Radio Based Approach for Channel Encoding and Decoding Using Forward Error Correction. *Wireless Personal Communications, 72*(4):2957–69. .10.1007/s11277-013-1191-z

Marriwala, N., Sahu, O. P., & Vohra, A. (2016a). Design of a Hybrid Reconfigurable Software Defined Radio Transceiver Based on Frequency Shift Keying Using Multiple Encoding Schemes. *Egyptian Informatics Journal*, *17*(1), 89–98. doi:10.1016/j.eij.2015.08.004

Marriwala, N., Sahu, O. P., & Vohra, A. (2016b). Novel Design of a Low Cost Flexible Transceiver Based on Multistate Digitally Modulated Signals Using Wi-Fi Protocol for Software Defined Radio. *Wireless Personal Communications*, *87*(4), 1265–1284. doi:10.1007/s11277-015-3052-4

Martinek, R., Al-Wohaishi, M., & Zidek, J. (2010). Software Based Flexible Measuring Systems for Analysis of Digitally Modulated Systems. *Roedunet International Conference (RoEduNet), 2010 9th* (pp. 397–402).

Mitola, J. (1999). Technical Callenges in the Globalization of Software Radio. *IEEE Communications Magazine*, *37*(February), 84–89. doi:10.1109/35.747254

Mitola, J., Bose, V., Leiner, B. M., Turletti, T., & Tennenhouse, D. (1999). Guest Editorial Software Radios. *IEEE Journal on Selected Areas in Communications*, *17*(4), 509–513. doi:10.1109/JSAC.1999.761032

Moir, T. J., & Pettigrew, A. M. (2014). A Multiplicative Cancellation Approach to Multipath Suppression in FM Radio. *Wireless Personal Communications*, *75*(2), 799–819. doi:10.1007/s11277-013-1392-5

Molla, D. M., Badis, H., George, L., & Berbineau, M. (2022). Software Defined Radio Platforms for Wireless Technologies. *IEEE Access: Practical Innovations, Open Solutions*, *10*, 26203–26229. doi:10.1109/ACCESS.2022.3154364

Molla, D. M., Badis, H., George, L., & Berbineau, M. (2022). Software Defined Radio Platforms for Wireless Technologies. *IEEE Access: Practical Innovations, Open Solutions*, *10*, 26203–26229. doi: 10.1109/ACCESS.2022.3154364

Molla, D. M., Badis, H., George, L., & Berbineau, M. (2022). Software Defined Radio Platforms for Wireless Technologies. *IEEE Access: Practical Innovations, Open Solutions*, *10*, 26203–26229. doi: doi:10.1109/ACCESS.2022.3154364

Noseworthy, J. (2007). Software-Defined Radios: The Radios of the Future. *Military Communications Conference, 2007. MILCOM 2007. IEEE* (pp. 18–21). IEEE.

Oza, J., Patel, Y., Trivedi, P., Ranpura, N., Patel, Z., Dalal, U., Jani, R., & Vijay, S. R. (2010). "Optimized Configurable Architecture of Modulation Techniques for SDR Applications. *International Conference on Computer and Communication Engineering, ICCCE'10* (pp. 11–13). IEEE. doi:10.1109/ICCCE.2010.5556800

Özyurt, S., Kucur, Oˇ., & Altunba¸s, I. (2007). Error Performance of Rotated Phase Shift Keying Modulation over Fading Channels. *Wireless Personal Communications*, *43*(4), 1453–1463. doi:10.1007/s11277-007-9319-7

Ramacher, U. (2007). Software-Defined Radio Prospects for Multistandard Mobile Phones. *IEEE Computer Society*, *40*(10), 62–69. doi:10.1109/MC.2007.362

Roth, J., Manjikian, N., & Sudharsanan, S. (2009). Performance Optimization and Parallelization of Turbo Decoding for Software-Defined Radio. *Canadian Journal Electrical Computing Enggineering, 34*(3).

Sadiku, M. N. O., & Akujuobi, C. M. (2004). Software-Defined Radio: A Brief Overview. *IEEE Potentials*, *23*(4), 14–15. doi:10.1109/MP.2004.1343223

Sadjadpour, H. (2000). Maximum a Posteriori Decoding Algorithms for Turbo Codes. *AeroSense 2000, Digital Wireless Communication II. Proceedings of the Society for Photo-Instrumentation Engineers*, *4045*, (pp. 73–83). doi:10.1117/12.394081

Sampaio, A. Z., Gomes, A. R., & Santos, J. P. (2012). Management of Building Supported on Virtual Interactive Models: Construction Planning and Preventive Maintenance. *Electronic Journal of Information Technology in Construction*, *17*, 121–133. doi:10.1016/j.aei.2006.09.003

Schiller, J. (2003). *Mobile Communications* (2nd ed.). Adison-Wesley.

Scotti, F., Laghezza, F., Ghelfi, P., & Bogoni, A. (2015). Multi-Band Software-Defined Coherent Radar Based on a Single Photonic Transceiver. *IEEE Transactions on Microwave Theory and Techniques*, *63*(2), 546–552. doi:10.1109/TMTT.2014.2386877

Scotti, F., Laghezza, F., Ghelfi, P., & Bogoni, A. (2015). Multi-band software-defined coherent radar based on a single photonic transceiver. *IEEE Transactions on Microwave Theory and Techniques*, *63*(2), 546–552. doi: doi:10.1109/TMTT.2014.2386877

Shannon, C. E. (1948). A Mathematical Theory of Communication. *The Bell System Technical Journal*, *27*(3), 379–423. doi:10.1002/j.1538-7305.1948.tb01338.x

Suihua University. (2005). Software Defined Radio: An Integrated Test Method for Designing Software Communications Architecture (SCA) Compliant Radios. *Microwave Engineering Europe,* 20–26.

Tribble, A. C. (2008). The Software Defined Radio: Fact and Fiction. *2008 IEEE Radio and Wireless Symposium* (pp. 5–8). IEEE. doi:10.1109/RWS.2008.4463414

Valenti, M. C., & Sun, J. (2001). The UMTS Turbo Code and an Efficient Decoder Implementation Suitable for Software-Defined Radios. *International Journal of Wireless Information Networks*, *8*(4), 203–215. doi:10.1023/A:1017925603986

Yarkan, S. (2015). A Generic Measurement Setup for Implementation and Performance Evaluation of Spectrum Sensing Techniques : Indoor Environments. *IEEE Transactions on Instrumentation and Measurement*, *64*(3), 606–614. doi:10.1109/TIM.2014.2355471

Zou, Q., Mikhemar, M., & Sayed, A. H. (2009). Digital Compensation of Cross-Modulation Distortion in Software-Defined Radios. *IEEE Journal of Selected Topics in Signal Processing*, *3*(3), 348–361. doi:10.1109/JSTSP.2009.2020266

CAN PROVIDE A COMPARISON IN TABULAR FORMAT OF THE WORD DONE PREVIOUSLY AND THE PROPOSED WORK

Table 5 represents the performance comparison between the proposed SDR Transceiver system using NI USRP for real-time data transfer for 4-bit QAM and state-of-the-art SDRs. Compared to SDRs presented in the literature, the proposed SDR Transceiver system closely adheres to the SDR concept by which most of the transceiver operation and radio hardware is configured through software programming in order to approximate a complete software-controlled operation based on a fully digital hardware architecture using NI USRP.

INTRODUCTION PART SHOULD BE IN DETAILED WAY

We have added more to the Introduction as discussed below:
The proposed SDR transceiver system can be used in real-time conditions for the transfer of the data in different forms such as binary codes or text and image. As the proposed system uses M-QAM for modulation of the data it shows a better performance for lower modulation order whereas the out gets inferior as we move to a higher order of 'M'. The proposed system uses FEC codes makes the system more secure and future-ready. The proposed SDR transceiver system uses decision-based carrier

Table 5. Performance comparison between the proposed SDR Transceiver system using NI USRP for real-time data transfer for 4-bit QAM and state-of-the-art SDRs

Ref. Features	Existing SDR Systems								Proposed SDR Systems
	(Roth et al. 2009)	(Zou et al. 2009)	(Martinek et al. 2010)	(Oza et al. 2010)	(Scotti et al. 2015)	(Kwag et al. 2015)	(Marimuthu et al. 2016)	(Fepeussi et al. 2019)	
Bandwidth	-	1GHz range	20 MHz	2.5GHz	2.53GHz	2.5GHz	2.0GHz	5GHz	10kHz- 10 GHz
SNR	-	27.5 dB	-	20dB	25dB	20dB	15dB	12dB	>10.2812dB
Data Rate(Mbps)	-		13	25	30	35		40	50
Application	-	-	Real measurement of error rate	Video. Image	Cognitive sensing	Wave Sensing	Near-Field Biomedical Imaging	Indoor Positioning	Wide Applications Real-Time/ Cognitive measurements
E_b/N_0 dB	2.7dB	-	28 dB(32-PSK);21 dB(64-QAM)	35 dB	-	-	-	-	14.3
BER	10^{-1}	10^{-4}	10^{-4}	10^{-4}	10^{-5}	10^{-5}	10^{-4}	10^{-5}	10^{-5}
Reliability	Less	-	-	High	High	High	High	High	Highly Reliable
Hardware Complexity	Complex	Less Complex	Complex	Low Bandwidth	Complex	Less Complex	Less Complex	Less Complex	Easy to Modify
Hardware Cost	High	Low	High	Low	Low	Low	Low	Low	Very Low
Hardware	-	-	-	-	PXIe-5451 AWG	-	Blade RF SDR (GNU Radio)	AD9361 SDR	USRP-2922
Modulation	QPSK	QPSK	M-QAM, M-PSK	FSK, QPSK	FMCW	-	SFCW	S-MFCW	Convolution, Turbo Coding
Coding Techniques	-	-	-	-	-	-	-	-	FEC Coding

tracking which ensures that phase tracking routine, the phase error, affected by the initial phase and frequency difference, is minimized and the received signal becomes a perfect reproduction of the transmitted signal except for the time delay. The biggest advantage of the proposed SDR transceiver system is that it is built as a reconfigurable system that can perform real-time signal processing. The proposed SDR transceiver system is generic in nature and offers a low-cost solution for secured transmission of data in real time. As the proposed SDR transceiver system runs on a generic platform it is easier to optimize the processing of the signal/data. In the proposed generic SDR transceiver system the complete processing of the Signal/data has been successfully performed through software. The dedicated hardware's used for testing the performance of the proposed SDR transceiver system; perform only the down conversion and digitization of a wide band of the RF spectrum. The proposed SDR helps to exploit the flexibility of signal/data processing through software thus helping to realize a system which could be modified dynamically at any stage through software.

Nikhil Marriwala (B-Tech., M-Tech. and PhD in Engineering & Technology) is working as Assistant Professor and Head of the Department Electronics and Communication Engineering Department, University Institute of Engineering and Technology, Kurukshetra University, Kurukshetra. He did his PhD. from National Institute of Technology (NIT), Kurukshetra in the department of Electronics and Communication Engineering. He did his post-graduation (M-Tech) in Electronics and Communication Engineering from Institute of Advanced Studies in Education (IASE) University, and did his B-Tech in Electronics and Instrumentation from MMEC, Mullana, Kurukshetra University, Kurukshetra. He has more than 19 years of experience teaching graduate and postgraduate students. More than 31 students have completed their M-Tech dissertation under his guidance. He has published more than 05 book chapters in different International books, has authored more than 10-books with Pearson, Wiley, etc. and has more than 40 publications to his credit in reputed International Journals (SCI, SCIE, ESCI, and Scopus) and 20 papers in International/National conferences. He has been granted 08 Patents with 02 Indian patents and 06 International Patents. He has been Chairman of Special Sessions in more than 22 International/National Conferences and has delivered a keynote address at more than 7 International conferences. He has also acted as organizing secretary for more than 05 International conferences and 01 National Conference. He has delivered more than 70 Invited Talks/ Guest Lectures in leading Universities/Colleges PAN India. He is having additional charge of Training and Placement Officer, UIET, Kurukshetra University, Kurukshetra and heading the T&P cell for more than 11 years now. He is the Single point of contact (SPOC) and head of local chapter of SWAYAM NPTEL Local Chapter of UIET, KUK. He is the SPOC for Infosys campus connect program for UIET, KUK. He is also the reviewer for many reputed journals such as the International Journal of Communication Systems, Wiley, IEEE Signal Processing Letters, International Journal of Measurement Technologies and Journal of Organizational and End User Computing (JOEUC), Egyptian Informatics Journal – Elsevier, Instrumentation Engineering (IJMTIE), International Journal of Interactive Communication Systems and Technologies (IJICST), Current Journal of Applied Science and Technology, UK. He has been awarded as the NPTEL ENTHUSIASTS for year 2019-2020 by NPTEL IIT, Madras. He has also been awarded as the "Career Guru of the Month" award by Aspiring Minds. His areas of interests are Software Defined Radios, Cognitive Radios, Soft Computing, Wireless Communications, Wireless Sensor Networks, Fuzzy system design, and Advanced Microprocessors.

C. Gnana Kousalya received the B.E.degree in Electronics and Communication Engineering from Government College of Technology,Coimbatore in the year 1993. She received the M.E.degree in Applied Electronics from Sathyabama University, Chennai in the year 2004 and Ph.D in Wireless Sensor Networks, from College of Engineering, Guindy, Anna University, Chennai. She has twenty five years of teaching and one year of industrial experience. She is a member of IEEE RAS, IEEE WIE & IEEE EMBS. She is also a corporate member of IETE and Life Member of ISTE. Her research interests include Wireless Sensor Networks, Image Processing and Signal processing.

B. Rajasekar is currently working as associate professor Department of Electronics and communication Engineering, Sathyabama Institute of Science and Technology, Chennai. He compleyed her B.E. ECE from Rajarajeswari engineering college, Chennai, He completed his post graduation in M.Tech- VLSI Design, He has completed his doctoral research in LDPC encoder and decoder, He has 15 years of teaching and research experience in Digital Signal Processing and Signals and systems. He has 35 publications of which 28 are indexed in Scopus and 7 are indexed in WoS.

N.M. Nandhitha is currently working as professor and Dean, School of Electrical and Electronics Engineering, Sathyabama Institute of Science and Technology, Chennai. She completed her B.E. ECE from Government College of Technology, Coimbatore. She completed her post graduation in M.E.Power Electronics and Industrial Drives by securing Gold Medal. She has completed her doctoral research in online weld monitoring by thermal imaging which is a project sponsored to the university from IGCAR, Kalpakkam. She has 24 years of teaching and research experience in Digital Image Processing and MATLAB programming. She has received and completed seven sponsored research projects in the above areas from BRNS, DST, TNSCST and BRFST. Currently she has three UBA projects to her credit. She has 150+ publications of which 88 are indexed in Scopus and 25 are indexed in WoS. She has published five monographs in the area of soft computing.She has delivered invited talks and Guest lectures in various other engineering colleges and universities. She has received best paper award three times and has also won CTS Best Teacher Award.

Ashu Gautamis has a B.Tech and M.tech in Instrumentation and Control and is Gold Medalist in Punjab Technicl Universityand has an enriching teaching and reserach experience of 16 years.She got three Interantional patents to her credit .She has published more than 15 reserach papers in Scopous SCI and ESCI .Three book chapters have been published with international reputed organization. She has been working as lead for various National and International Workshops conducted in Univeristy and has been leading the admission stratergy of University for School of Engineering in her Univeristy.

Aarti Sangwan obtained her B. Tech in Computer Science and Engineering from Rajasthan Technical University, Kota, India. She secured her M. Tech in Computer Science and Engineering from Amity University, Noida, Uttar Pradesh, India. She completed her Ph.D. in Computer Science and Engineering from Mody University of Science and Technology, Lakshmangarh, Rajasthan, India. Dr. Aarti is currently working as an Assistant Professor in the Department of Computer Science and Information Technology at the Central University of Haryana, Mahendergarh. She is in teaching profession for more than one year. She has published 14 papers in National and International Journals, Conferences and Symposiums and 5 patents. Her research areas include Data Science, Wireless Sensor Networks and Body Area Networks.